Pyrroloquinoline Quinone Biogenesis: Characterization of PqqC and Its H84N and H84A Active Site Variants†

Olafur Th. Magnusson,‡,§,|| Jordan M. RoseFigura,‡,§ Hirohide Toyama,⊥,△ Robert Schwarzenbacher,# and Judith P. Klinman*,§

Department of Chemistry and Department of Molecular and Cell Biology, University of California, Berkeley, California 94720, Department of Biological Chemistry, Faculty of Agriculture, Yamaguchi University, Yamaguchi 753-8515, Japan, and Department of Molecular Biology, Division of Structural Biology, Universität Salzburg, 5020 Salzburg, Austria

Received January 25, 2007; Revised Manuscript Received March 26, 2007

ABSTRACT: Pyrroloquinoline quinone [4,5-dihydro-4,5-dioxo-1*H*-pyrrolo[2,3-*f*]quinoline-2,7,9-tricarboxylic acid (PQQ)] is a bacterial vitamin that serves as a cofactor in numerous alcohol dehydrogenases. Its biosynthesis in *Klebsiella pneumoniae* is facilitated by six genes, *pqqABCDEF*, and proceeds by an unknown pathway. The protein encoded by *pqqC* catalyzes the final step of PQQ formation, which involves a ring closure and an overall eight-electron oxidation of 3a-(2-amino-2-carboxyethyl)-4,5-dioxo-4,5,6,7,8,9-hexahydroquinoline-7,9-dicarboxylic acid (AHQQ) in the absence of a redox-active metal or cofactor. A recent crystal structure has implicated numerous PQQ−PqqC interactions [Magnusson et al. (2004) *Proc. Natl. Acad. Sci. U.S.A. 101*, 7913−7918]. To investigate the mechanism of the PqqC reaction, the active site residue His84 has been mutated to H84A and H84N, and the kinetic and spectroscopic properties have been compared to each other and the wild-type enzyme using aerobic and anaerobic conditions. Both mutants form PQQ under aerobic conditions with rate constants of 0.09 min^{-1} and 0.056 min^{-1} relative to 0.34 min^{-1} for the wild-type enzyme. In addition to the initial E−AHQQ complex (532−536 nm) and the product E−PQQ complex (346−366 nm), a number of spectral intermediates are observed between 316 and 344 nm. The anaerobic reaction is particularly informative, showing that while mixing of H84N with AHQQ leads to a 344 nm intermediate, this is unable to proceed to a final 318 nm species; by contrast H84A forms the 344 nm species as a precursor to the 318 nm species. In the context of the proposed chemical mechanism for PqqC [Magnusson et al. (2004) *Proc. Natl. Acad. Sci. U.S.A. 101*, 7913−7918], we assign the 344 nm intermediate to a quinoid species and the 318 nm intermediate to an initial quinol species. The proposed role of H84 is as a proton donor to the oxyanion of the quinoid species such that subsequent C−H bond cleavage can occur to form a monoanionic quinol. In the absence of a proton donor (as occurs in H84N), the normal reaction path is precluded as this would require formation of an unstable, dianionic species. Unlike H84N, H84A appears to be small enough to allow entry of active site water, which is postulated to adopt the role of active site proton donor.

Pyrroloquinoline quinone [4,5-dihydro-4,5-dioxo-1*H*-pyrrolo[2,3-*f*]quinoline-2,7,9-tricarboxylic acid (PQQ)[1] (Scheme 1)] is an aromatic, tricyclic *o*-quinone that serves as cofactor for a number of prokaryotic dehydrogenases, largely from Gram-negative bacteria. The oxidative reactions catalyzed by PQQ−enzymes are involved in catabolic pathways, where the best studied examples are methanol dehydrogenase and glucose dehydrogenase (*1*, *2*). PQQ belongs to a family of quinone cofactors that has been recognized as the third class of redox cofactors following pyridine nucleotide- and flavin-dependent cofactors (*3*). Although plants and animals do not produce PQQ, the cofactor has invoked considerable interest because of its presence in human milk and its antioxidant properties (*4*−*6*). Recently, a claim was put forth for the occurrence of a PQQ-dependent enzyme in mammals. The enzyme, aminoadipic 6-semialdehyde dehydrogenase (AASDH), is involved in the breakdown of lysine, the level of which was depressed in mice fed a PQQ-deficient diet (*7*).

Scheme 1: The Carbon and Nitrogen Atoms of PQQ Originate from a Glutamate and a Tyrosine Residue

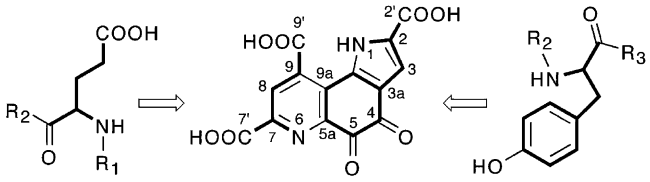

† This work was supported by the National Institutes of Health (Grant GM39296 to J.P.K.). O.T.M. was supported by a Miller Fellowship grant. R.S. was supported by grants from the Austrian Science Fund (P18702) and OeNB Anniversary Fund (ONB12074).

* To whom correspondence should be addressed. E-mail: klinman@berkeley.edu. Tel: 510-642-2668. Fax: 510-643-6232.

‡ These authors contributed equally to this work.

§ University of California, Berkeley.

|| Present address: decode Genetics, Sturlugata 8, IS-101 Reykjavik, Iceland.

⊥ Yamaguchi University.

△ Present address: University of Ryukyus, Okinawa, Japan.

Universität Salzburg.

[1] Abbreviations: PQQ, pyrroloquinoline quinone; DCIP, dichloroindole phenol; PMS, phenazine methosulfate; NTA, nitriloacetic acid; AHQQ, 3a-(2-amino-2-carboxyethyl)-4,5-dioxo-4,5,6,7,8,9-hexahydroquinoline-7,9-dicarboxylic acid; PMSF, phenylmethanesulfonyl fluoride; AASDH, aminoadipic 6-semialdehyde dehydrogenase.

10.1021/bi700162n CCC: $37.00
Published on Web 05/25/2007

Scheme 2: The PqqC Reaction[a]

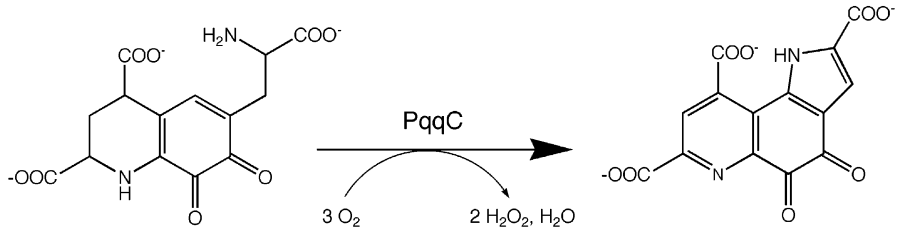

[a] This reaction involves an overall eight-electron oxidation, leading to a pyrrole and pyridine ring, and has previously been shown to consume 3 mol of O_2 per product formed.

Scheme 3: Proposed Mechanism of PqqC[a]

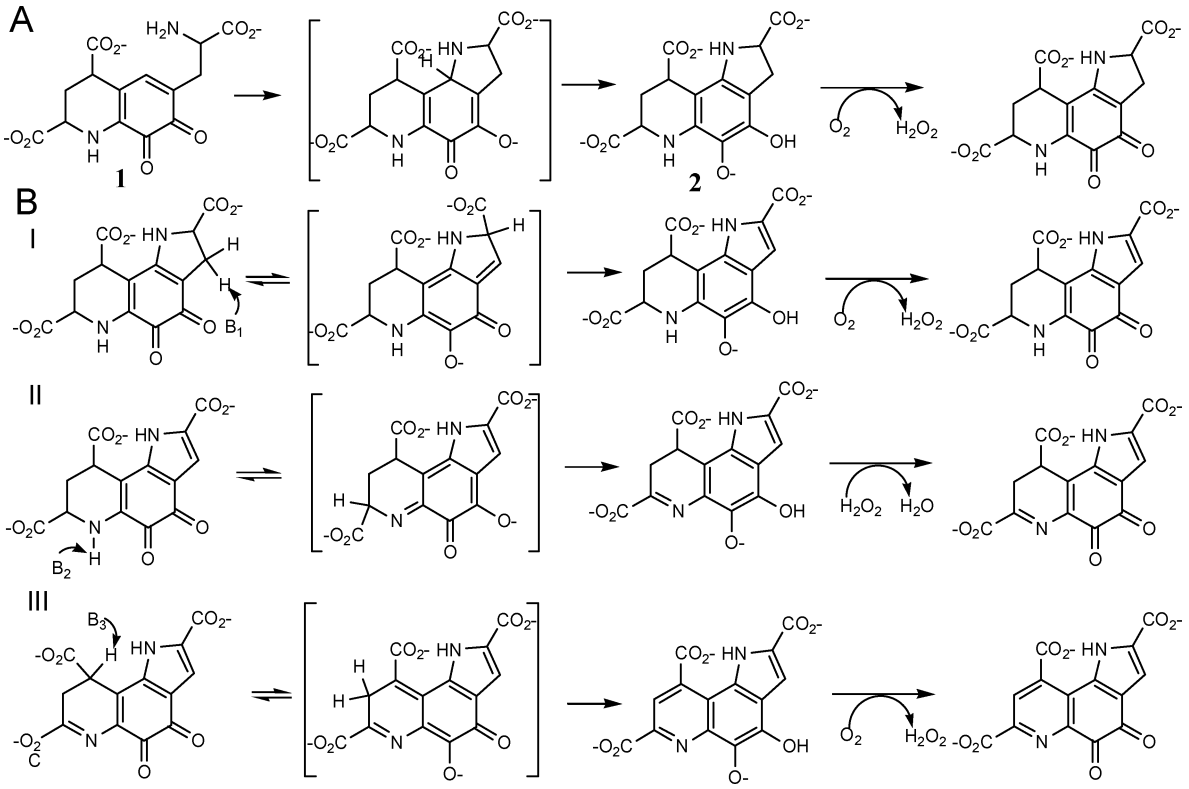

[a] Note that steps I−III are shown in random order. B1, B2, and B3 denote residues proposed to act as base catalysts in the respective tautomerization reactions.

However, the sequence homology approach that was used to relate PQQ−enzymes to AASDH is reported to have been erroneously obtained (*8*). Thus, until a mammalian AASDH is purified and characterized, the claim for PQQ as a vitamin in mammals should be considered premature.

The biosynthesis of PQQ is an intriguing process, whereby all carbon and nitrogen atoms of the cofactor are derived from two amino acids, tyrosine and glutamate (*9*) (Scheme 1). Genetic and isotope labeling studies strongly suggest that a peptide containing highly conserved Glu and Tyr residues serves as the precursor to PQQ (*2*, *10*). The mechanism(s) by which the processing of this peptide yields the active cofactor is (are) currently unknown. With the goal of elucidating the enzymatic steps involved in PQQ biosynthesis, we are currently working toward characterizing each of the gene products in this pathway. PQQ biosynthesis in *Klebsiella pneumoniae* requires the expression of six genes, designated *pqqABCDEF* (*11*). The final step in the pathway is catalyzed by PqqC (*12*, *13*), and we have recently shown that this reaction involves a ring cyclization of 3a-(2-amino-2-carboxyethyl)-4,5-dioxo-4,5,6,7,8,9-hexahydroquinoline-7,9-dicarboxylic acid, together with an eight-electron oxidation to produce PQQ (*14*, *15*) (Scheme 2). The X-ray crystal structure of PqqC in native form and with PQQ bound in the active site has recently been solved (*15*, *16*). The enzyme is a 58 kDa homodimer where each monomer comprises a seven helix bundle fold, which undergoes a major conformational change upon binding of PQQ (*15*).

The active site of PqqC has a number of basic residues, which are postulated to stabilize the three negatively charged carboxylate ions of AHQQ and to function in catalysis (*15*). In particular, the proposed mechanism of the enzyme involves the action of three conserved basic residues (Scheme 3), which have been tentatively assigned to H24, H84, and H154 (*15*). Herein we describe the kinetics of the single-turnover reaction of WT enzyme and two active site H84 mutants (H84N and H84A), including the spectroscopic detection of intermediates that provide insight into the catalytic mechanism of PqqC. We have also measured the binding of PQQ to WT enzyme and the H84 mutants and, in conjunction with assays performed at low enzyme concentration, conclude that tight binding of PQQ results in

severe product inhibition of the reaction. The latter may explain why previous studies were unable to detect multiple enzyme turnovers (*15*, *17*).

MATERIALS AND METHODS

Chemicals, Reagents, and Molecular Biology Products. Buffers, salts, general reagents, and culture media were obtained from Sigma and Fisher and were of the highest available purity. Dichloroindole phenol (DCIP), phenazine methosulfate (PMS), Q-Sepharose, SP-Sepharose, and phenyl-Sepharose resins were from Sigma. PQQ (>99%) was from Fluka. The concentration of PQQ in aqueous solution was determined spectrophotometrically as described elsewhere (*18*). Ni-nitriloacetic acid (NTA) resin, DNA purification kits, and PCR primers were purchased from Qiagen. Enzymes and reagents for PCR reactions were from Roche, including Expand High Fidelity DNA polymerase. Restriction enzymes and appropriate reaction buffers were purchased from New England Biolabs. Bugbuster reagent, benzonase, T4 DNA ligase, cell lines, vectors for cloning and expression, and sequencing primers were obtained from Novagen. AHQQ was purified from a *ppqC* mutant strain EMS12 of *Methylobacterium extorquens* (*13*) as described elsewhere (*14*). Concentration of AHQQ was determined spectrophotometrically at pH 7 by averaging the concentrations determined at three wavelengths with the following extinction coefficients (*15*): $\epsilon_{222} = 15.7\ mM^{-1}\ cm^{-1}$, $\epsilon_{274} = 8.26\ mM^{-1}\ cm^{-1}$, and $\epsilon_{532} = 2.01\ mM^{-1}\ cm^{-1}$. Plasmid (pBCP-165) containing all of the genes in the PQQ operon of *K. pneumoniae* was a generous gift from Professor Robert Rucker, University of California, Davis. This plasmid was originally made in the laboratory of Professor Peter W. Postma, University of Amsterdam, The Netherlands (*11*, *12*). An *Escherichia coli* recombinant strain pGP492, harboring the gene for soluble glucose dehydrogenase (sGDH) from *Acinetobacter calcoaceticus*, is from the laboratory of Professor Hirohide Toyama, Yamaguchi University, Japan.

PCR Cloning and Expression. PCR cloning was performed using the following primers: pqqC/D-1, 5′-GGCATTACATATGCTGATCACTGACACGCTGTCGCCGC-3′; pqqC/D-2, 5′-GACCGCTCGAGTTACTCTGGCTCACGGCAGGTGATCCACTT-3′. Underlined sequences are restriction sites for *Nde*I and *Xho*I, respectively, that were designed for subsequent cloning. The reaction mixture contained 10 mM Tris buffer, pH 8.3, 50 mM KCl, 2.5 mM $MgCl_2$, 200 μM dNTPs, 2 μM primers, 70 ng/μL pBCP-165, and 3.5 units/μL DNA polymerase. Reaction conditions: melting, 95 °C; annealing, 55 °C; elongation, 72 °C. Each step was 1 min for a total of 35 cycles. The purified PCR product was digested with *Nde*I and *Bam*HI, followed by ligation into pET-24b for generation of wild-type PqqC. After transformation into NovaBlue cells, screening for positive colonies was done by plasmid purification and restriction analysis of clones. The isolated plasmid named pET-24b-pqqC/D was sequenced from both directions using the T7 promoter and terminator primers, respectively. The H84N mutant gene is on pET-21d plasmid (*Eco*RI/*Xho*I), contains a C-terminal His tag, and confers resistance to ampicillin. The following primers were used for Quickchange PCR mutagenesis: H84Nf, 5′-GCATCCTCGACAACGACGGCAGCCAC-3′; H84Nr, 5′-GTGGCTGCCGTCGTTGTCCAGGATCC-3′. The H84A mutation is on a pET-24b pqqC plasmid that contains a C-terminal His tag and confers resistance to kanamycin. Mutagenesis of H84A was performed using a commercial kit (Stratagene), and the following primers were used: H84Af, 5′-CGGATCCTCGACGCCGACGGCAGCCAC-3′; H84Ar, 5′-GTGGCTGCCGTCGGCGTCGAGATCCG-3′.

Expression of plasmids was done using BL21(DE3) cells in LB medium supplemented with 50 μg/mL kanamycin (WT and H84A) or 100 μg/mL ampicillin (H84N). Cultures were grown at 37 °C to an optical density at 600 nm of ~0.8, at which time IPTG (1 mM) was added, and the cells were harvested ~4 h later. Both pET-24b-pqqC/D and pET-28b-pqqC/D produced high quantities of WT protein as judged by SDS−PAGE analysis. Solubility tests using Bugbuster reagent in the presence of 0.2 M potassium phosphate, pH 8, showed that ~50% of the protein was soluble with the remainder presumably as insoluble inclusion bodies. Considerably lower expression of the H84 mutants was observed; however, most of the protein remained soluble after cell lysis with the addition of ~0.9 M KCl in the lysis buffer.

Purification of Wild-Type PqqC. Cells harboring pET-24b-pqqC/D (~30 g) were resuspended in 0.2 M potassium phosphate buffer, pH 8, containing 1 mM DTT, 1 mM PMSF, and 1 mM EDTA. Cell lysis was performed by sonication using a Branson sonifier with output setting at 8 and duty cycle at 30% (3 × 5 min). Lysed cells were centrifuged, and the clear supernatant was diluted 5-fold with 20 mM Tris, pH 8, and 1 mM DTT (buffer A). The diluted sample was applied to a Q-Sepharose column (2.5 × 30 cm, flow rate = 1.7 mL/min), equilibrated in buffer A, followed by a buffer wash (~150 mL). PqqC was eluted with a gradient of 0−300 mM KCl in buffer A (2 L total volume), and the collected fractions were analyzed by SDS−PAGE, followed by concentration of PqqC-containing fractions (Amicon YM10). The protein was further purified by size-exclusion chromatography using an Ultrogel AcA54 column (2.5 × 110 cm, flow rate = 0.3 mL/min) in 100 mM potassium phosphate buffer, pH 8 (buffer B). PqqC-containing fractions were pooled on the basis of SDS−PAGE analysis, and the protein was subsequently concentrated using an Amicon YM10 ultrafiltration device followed by freezing in liquid nitrogen and storage at −80 °C. A sample of purified protein was sent to the AAA Service Laboratory, Boring, OR, for quantitative amino acid analysis. Triplicate analysis of the protein in conjunction with UV−vis absorption of the same sample yielded an extinction coefficient of $\epsilon_{280} = 2.06\ (mg/mL)^{-1}$, or $59.6\ mM^{-1}\ cm^{-1}$. WT protein with an N-terminal His tag (pET-28b-pqqC/D) was not purified.

Purification of H84N and H84A. Cells (~25 g) were resuspended in buffer C (0.2 M potassium phosphate, pH 8, 300 mM NaCl, 10 mM imidazole, 10 mM β-mercaptoethanol) augmented with 1 mM EDTA, 0.5 mM PMSF, and 0.9 M KCl. After sonication and centrifugation as described for WT the clear supernatant was applied to a 10 mL Ni-NTA column that had been equilibrated in buffer C. After a buffer wash the His-tagged bound protein was eluted with buffer C supplemented with 300 mM imidazole. Fractions containing mutant enzyme were analyzed by SDS−PAGE, pooled, concentrated, and further purified by size-exclusion chromatography as described above for the WT protein. Due to precipitation at higher concentrations, H84A could only be concentrated to approximately 55 μM.

Expression and Purification of sGDH. The apo form of sGDH was expressed and purified with a simplified modification of literature procedures (*19*). Instead of using a fermentor, overnight cultures (18 L) in shaker flasks were employed. Cells (~80 g) were disrupted by sonication in 250 mL of 0.1 M Tris, pH 7.5, 0.2 M NaCl, 3 mM $CaCl_2$, 0.5 mM PMSF, and 1000 units of benzonase. After centrifugation, the clear supernatant was dialyzed overnight against 20 mM Tris, pH 7.5, and 3 mM $CaCl_2$ (buffer D). The dialysate was passed through an SP-Sepharose column (2.5 × 30 cm), and after a buffer wash, sGDH was eluted with a NaCl gradient (0−450 mM) in buffer D. Fractions containing sGDH were assayed as described elsewhere (*19*), pooled on the basis of enzyme activity, and concentrated to ~20 mL. Tris buffer, pH 7.5, was added to a final concentration of 0.1 M and solid $(NH_4)_2SO_4$ to a final concentration of 1 M, and the protein solution was passed over a phenyl-Sepharose column (1.5 × 20 cm). The protein was eluted by a gradient (500 mL) of decreasing concentration of $(NH_4)_2SO_4$ (1 M to 0). Enzyme-containing fractions based on activity assays were combined and dialyzed against buffer D overnight. The purified protein was concentrated by ultrafiltration (Amicon YM10), frozen in liquid nitrogen, and stored at −80 °C. This procedure yielded ~20 mg of protein with specific activity of ~7000 units/mg, which is comparable to that reported in the literature (*19*).

Single-Turnover Kinetics. The 100 μM enzyme (WT or H84N) or 50 μM (H84A) was mixed with substrate, AHQQ (40 or 4.6 μM, respectively), in 100 mM potassium phosphate buffer, pH 8.0, in a total volume of 100 μL. The mixture was transferred to a microcuvette, and UV−vis spectra were recorded within 20 s of mixing. Spectra were obtained on a HP-8452A diode-array spectrophotometer, and the temperature of the reaction was maintained at 20 °C using a circulating water bath. Spectra were acquired at predetermined time points and the data exported to SPECFIT/32 for analysis. A control sample, containing enzyme only, was also measured under identical conditions. The spectra obtained in this manner were subtracted from spectra at the same time points during the enzymatic reaction. The control run was necessary to correct for absorption due to light scatter resulting from some protein precipitation during the course of the reaction.

Anaerobic reactions were done under the same conditions as described above. Enzyme and substrate were made anaerobic by repeated cycles of argon purging and high-vacuum evacuation on a Schlenk line. The sealed samples were brought into an anaerobic chamber, the protein was transferred into a microcuvette fitted with a rubber stopper, and the substrate was loaded into a syringe and the needle inserted through the stopper and into the top of the cuvette. The cuvette with the syringe attached was brought out to the spectrophotometer, and the substrate was mixed thoroughly with enzyme before spectra were recorded. After some time, when no further changes were observed in the UV−vis spectrum of the samples, the stopper was removed, and air was blown over the surface of the sample for a few seconds, demonstrating product formation in all cases.

Binding Assay for PQQ. Binding of PQQ to PqqC (WT and H84N) was measured fluorometrically. Assays were done in 100 mM potassium phosphate buffer, pH 8.0 at 25 °C. A fixed concentration of PQQ (ligand) was employed (50 nM for WT and 20 nM for H84N), and the concentration of enzyme was varied. Samples were incubated for 30 min and fluorescence emission spectra recorded (slit width 10 nm) with an excitation wavelength at 365 nm (slit width 5 nm) and 0.2 s integration time. Data were fitted to a quadratic binding isotherm (eq 1), where ΔF equals the change in fluorescence in a given sample compared to free ligand, ΔF_M equals the change in fluorescence at saturation, $[E]_T$ equals the total concentration of enzyme in each sample, $[L]_T$ equals the concentration of total ligand, and K_D is the dissociation constant of the enzyme−ligand complex. Data fitting was done using Kaleidagraph (Synergy Software).

$$\Delta F = \Delta F_M[([E]_T + [L]_T + K_D) - (([E]_T + [L]_T + K_D)^2 - 4[E]_T[L]_T)^{0.5}/(2[L]_T)] \quad (1)$$

PqqC Assays by Activation of sGDH. PqqC was assayed in a similar fashion as described elsewhere (*17*). PqqC was mixed with AHQQ in 100 mM potassium phosphate buffer, pH 8.0 at 25 °C. Aliquots (30 μL) were withdrawn at different time points and mixed with 10 μL of 4 M HCl to quench the reaction followed by immediate freezing in liquid nitrogen and storage until quantitation of PQQ. The amount of PQQ produced in the reaction was determined using the method of Matsushita et al. (*20*), which involves PQQ-dependent activation of the apo form of sGDH. Assays were done in 60 mM PIPES buffer, pH 6.5, 3 mM $CaCl_2$, and 0.1% Triton X-100 at 25 °C in a total volume of 1 mL. sGDH (10 μL, 400 nM) and 10 μL of PQQ (0.01−0.25 nM) or 10 μL of PqqC reaction mixture were added to the buffer and preincubated for 5 min, followed by addition of glucose (50 mM), PMS (0.5 mM), and DCIP (0.1 mM). The reaction was monitored by the decrease in absorbance at 600 nm due to reduction of DCIP. A small decrease in absorbance at 600 nm was observed without addition of PQQ, and this value was subtracted from all subsequent measurements. A linear response in the activity of sGDH was observed with regard to the concentration of PQQ, which allowed for the construction of a standard curve used for PQQ quantitation in the PqqC reaction (see Supporting Information).

RESULTS

Expression and Purification of Proteins. PqqC from *K. pneumoniae* has been successfully cloned and expressed in *E. coli*. Purification of the wild-type enzyme involves a two-step chromatographic procedure involving anion-exchange chromatography followed by size exclusion. The purity of the isolated protein was judged to be ≥95% based on SDS−PAGE analysis (Figure 1). The overall yield of protein for this procedure was ~25 mg/L of culture. In single-turnover studies PqqC behaved identically to PqqC carrying a His tag, which has been previously prepared and used in published structural studies (*15*, *16*). The decision was therefore made to construct all subsequent mutants with His tags for the purpose of rapid purification. In addition, the His-tag form of the enzyme appears to be somewhat more soluble than the native enzyme. The H84N and H84A mutants were purified by affinity chromatography on a nickel column followed by size-exclusion chromatography. The expression for these mutants was lower than WT and yielded ~3 mg/L of culture.

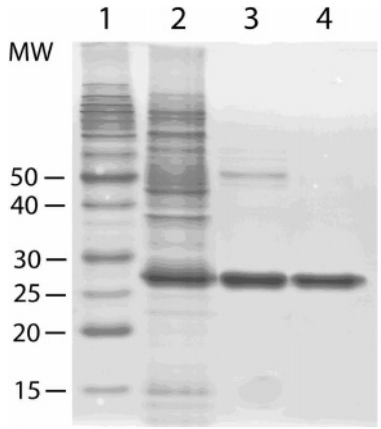

FIGURE 1: SDS−PAGE gel showing the purification of WT-PqqC from *K. pneumoniae* expressed in *E. coli*. Lanes: 1, markers; 2, crude extract after sonication and centrifugation; 3, pooled fractions following anion-exchange chromatography using Q-Sepharose; 4, pooled and concentrated fractions following size-exclusion chromatography using Ultrogel AcA54. Purified PqqC migrates as an ~28 kDa protein in accordance with its calculated molecular mass of 28.9 kDa.

Single-Turnover Kinetics of WT, H84N, and H84A. The rate of the reaction catalyzed by PqqC is slow, displaying a first-order rate constant of ~0.4 min^{-1} under single-turnover conditions using an assay based on quantitation of PQQ by HPLC (*15*). The substrate, AHQQ, has a wine red color due to a distinct quinonoid transition with λ_{max} at 532 nm, and the product, PQQ, also has multiple transitions in the UV−vis range, including a band at 331 nm (*14*). These properties make this system ideal to probe for spectral changes during the course of the reaction. Reactions were done with excess enzyme over substrate (2.5 equiv) to simplify the kinetics by ensuring that all substrate was in the E−S complex. Spectra at various time points during the WT-PqqC reaction are shown in Figure 2A. Qualitative assessment of the data shows the rapid decay of substrate at 532 nm, concomitant with the appearance of a chromophore with λ_{max} at 316 nm (WT-I). This species subsequently decays, and a direct precursor−product relationship with a new chromophore with λ_{max} at 346 nm can be seen by the isosbestic point at 332 nm. The final chromophore represents enzyme-bound PQQ (WT-PQQ) as determined by comparison to the spectrum of a sample of PqqC with enzyme after the addition of authentic PQQ (data not shown). The spectrum of enzyme-bound PQQ is red shifted by about 15 nm compared to the free cofactor (Table 1). Data at single wavelengths (Figure 2B) can be fit directly to a process involving three enzyme-bound species; however, a more accurate analysis was obtained by global fitting of the data using the program SPECFIT/32. Singular-value decomposition analysis yielded each individual spectral component, and the data were fit to an irreversible, two consecutive exponential model, which yielded first-order rate constants $k_1 = 0.960$ (±0.013) min^{-1} and $k_2 = 0.340$ (±0.005). Compilation of the results obtained from the global fitting procedure are shown in Table 1. A more detailed summary of the data, including all recorded spectra, deconvoluted spectra of each component, and the concentration profiles during the reaction can be found in Supporting Information.

Single-turnover studies were also performed with the active site variants, H84N and H84A, under identical conditions

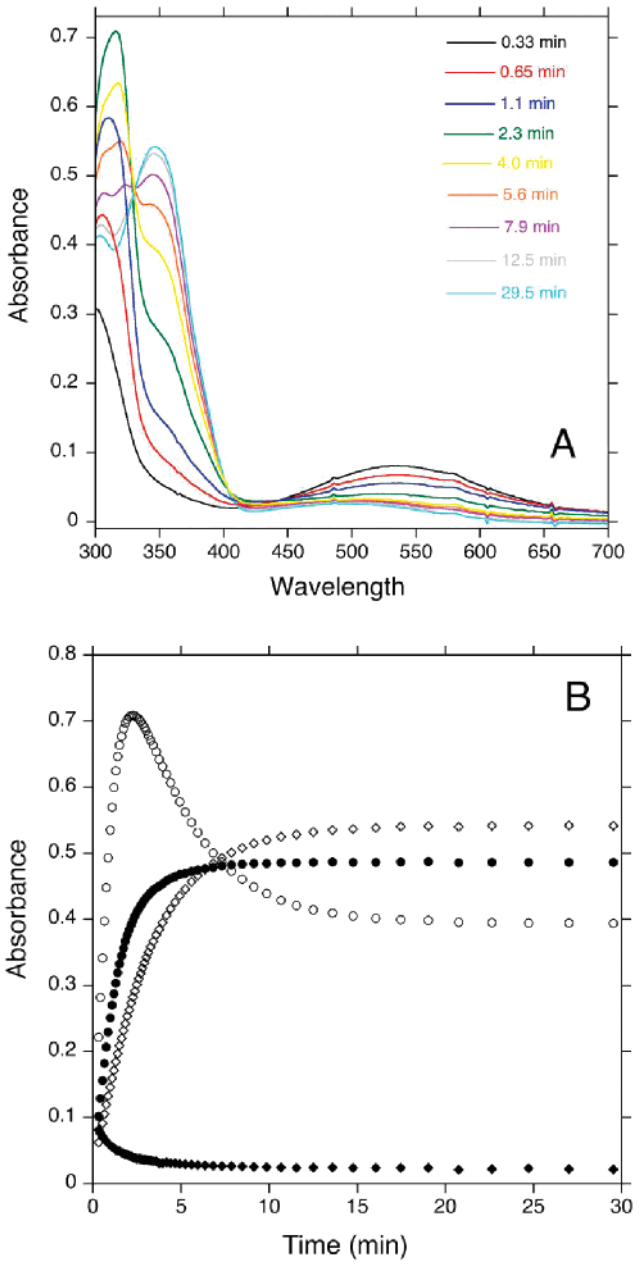

FIGURE 2: Spectral changes during the WT-PqqC reaction under single-turnover conditions at 20 °C. (A) Nine representative spectra at the indicated time points (0.33, 0.65, 1.1, 2.3, 4.0, 5.6, 7.9, 12.5, and 29.5 min, respectively). A total of 59 scans were acquired in the experiment. (B) Spectral traces at four single wavelengths, representative of different species or processes during the reaction. Closed diamonds (◆) show changes at 536 nm, representing disappearance of substrate. Open circles (○) show changes at 316 nm, representing formation and dissipation of an intermediate (WT-I). Closed circles (●) show changes at 332 nm, which is the isosbestic point between WT-I and product. Open diamonds (◇) show changes at 346 nm, which represents the final enzyme−PQQ complex.

Table 1: Results from Global Fitting (SPECFIT/32) of Spectral Changes during the Aerobic WT-PqqC Reaction

species[a]	λ_{max} (nm)	ϵ ($mM^{-1}\,cm^{-1}$)[c]	rate constant (min^{-1})
WT-AHQQ	536	2.0	
WT-I	316	23	$k_1 = 0.960$ (±0.013)
WT-PQQ	346, 498	12, 0.6	$k_2 = 0.340$ (±0.005)
PQQ[b]	331, 475	10, 0.7	

[a] The WT prefix refers to enzyme-bound species. [b] From ref *27*. [c] Values for ϵ are within 3%.

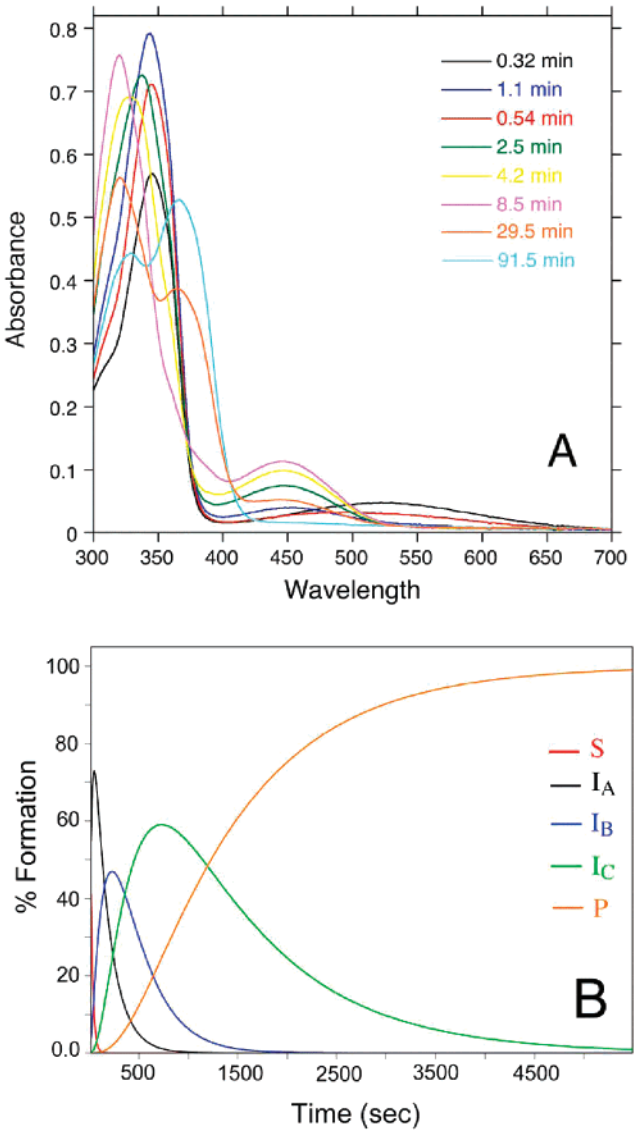

FIGURE 3: Single-turnover reaction of the active site variant H84N. (A) Representative spectra during the reaction at the following time points: 0.32, 0.54, 1.1, 2.5, 4.2, 8.5, 29.5, and 91.5 min, respectively. A total of 251 spectra were recorded for the reaction (see Supporting Information). (B) Percentage concentration profile as determined by global fitting of the five enzyme-bound species observed in the reaction. Key: S is substrate; I_A is first intermediate; I_B is second intermediate; I_C is third intermediate; P is product.

Table 2: Results from Global Fitting (SPECFIT/32) of Spectral Changes in the Aerobic Reaction of H84N

species[a]	λ_{max} (nm)	ϵ ($mM^{-1}\,cm^{-1}$)[c]	rate constant[d] (min^{-1})
H84N-AHQQ	532	2.1	
H84N-I_A	344	20	$k_1 = 2.75$ ($\pm$0.04)
H84N-I_B	330, 448	15, 2.7	$k_2 = 0.378$ ($\pm$0.022)
H84N-I_C	320, 445	20, 3.0	$k_3 = 0.218$ ($\pm$0.006)
H84N-PQQ	366, 329	11, 9.2	$k_4 = 0.0562$ ($\pm$0.0005)
PQQ[b]	331, 475	10, 0.7	

[a] H84N prefix refers to enzyme-bound species. [b] From ref *27*. [c] Values for ϵ are within 5%. [d] Rate constant for formation of species.

as described for the WT enzyme. Representative spectra during the course of the reaction are shown in Figure 3A (H84N) and Figure 4A (H84A). The overall reaction is slower than for WT enzyme, and the spectral changes during the H84N reaction can be described involving either four or

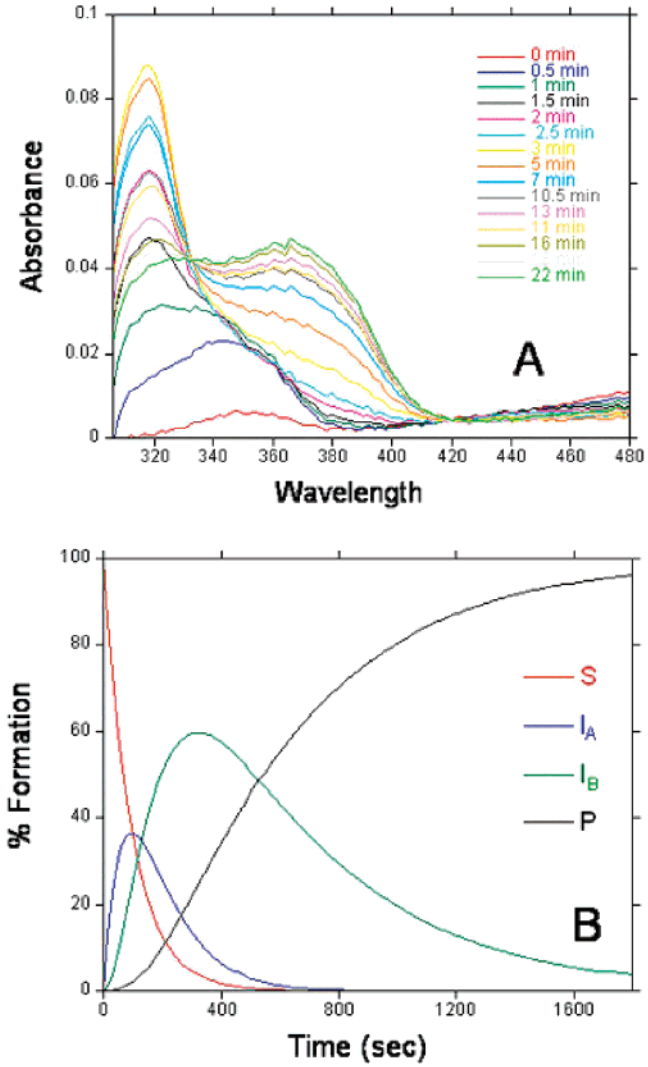

FIGURE 4: Single-turnover reaction of the active site variant H84A. (A) Representative spectra during the reaction at the following time points: 0, 0.5, 1, 1.5, 2, 2.5, 3, 5, 7, 10.5, 11, 13, 16, 18, and 22 min, respectively. A total of 251 spectra were recorded for the reaction. (B) Percentage concentration profile as determined by global fitting of the four enzyme-bound species observed in the reaction. Key: S is substrate; I_A is first intermediate; I_B is second intermediate; P is product.

Table 3: Results I_A from Global Fitting (SPECFIT/32) of Spectral Changes during the Aerobic H84A Reaction

species[a]	λ_{max} (nm)	ϵ ($mM^{-1}\,cm^{-1}$)[c]	rate constant[d] (min^{-1})
H84A-AHQQ	532	2.1	
H84A-I_A	344	5.9	$k_1 = 0.90$ ($\pm$0.19)
H84A-I_B	318	37	$k_2 = 0.57$ ($\pm$0.08)
H84A-PQQ	366, 329	9.5, 0.7	$k_3 = 0.09$ ($\pm$0.00)
PQQ[b]	331, 475	10, 0.7	

[a] H84A prefix refers to enzyme bound species. [b] From ref *27*. [c] Values for ϵ are within 10%. [d] Rate constant for formation of species.

five different species. The global fit is slightly better using five species, as determined by the residuals of the fit and by visual assessment of the quality of fits at single wavelengths. A summary of global fitting using an irreversible, four consecutive exponential model is shown in Table 2 for H84N, and the concentration profile obtained by the fit is shown in Figure 3B. A detailed comparison of a three-exponential versus the four-exponential model is given in Supporting Information. The final enzyme-bound product

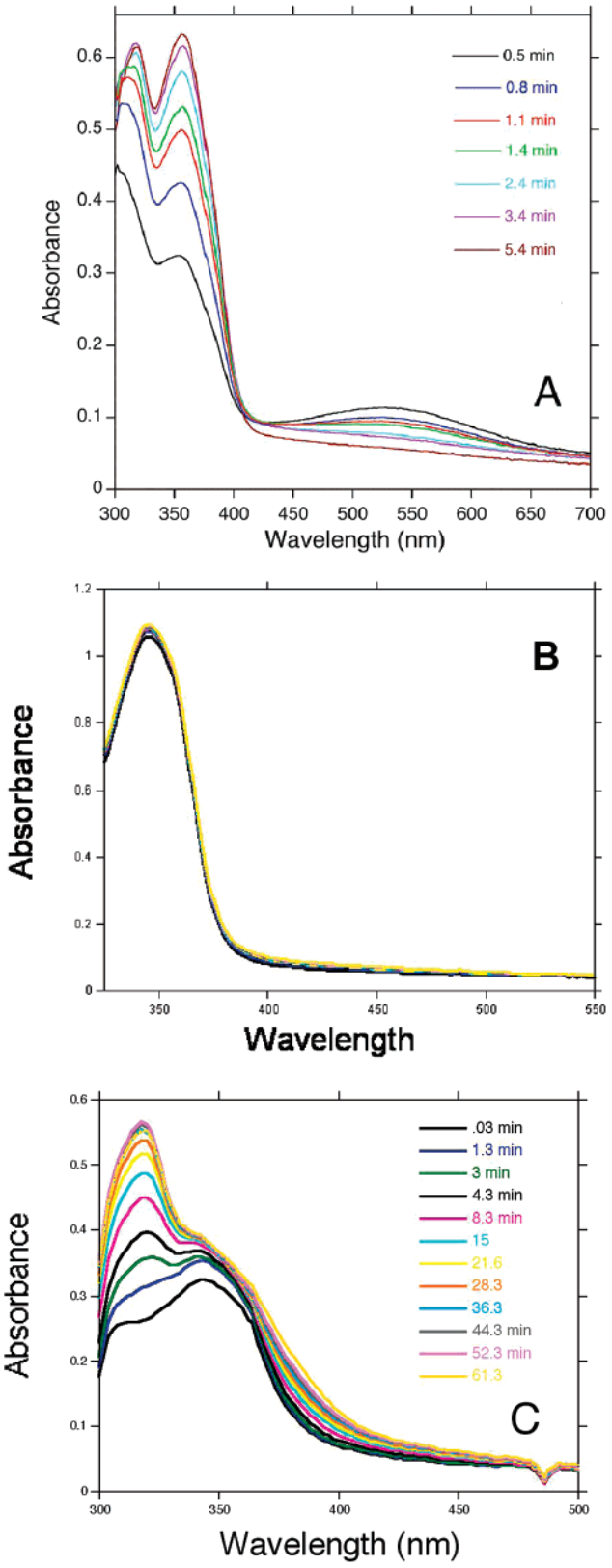

FIGURE 5: Spectra obtained in the PqqC reaction under anaerobic conditions with WT (A), H84N (B), and H84A (C). Representative spectra for the WT reaction are shown at the following time points: 0.5, 0.8, 1.1, 1.4, 2.4, 3.4, and 5.4 min. The WT data (A) show the appearance of two intermediates at 318 and 356 nm. The H84N data (B) show the time course for the anaerobic reaction and the buildup of a single intermediate at 344 nm. The H84A representative spectra are shown at 0.3, 1.3, 3, 4.3, 8.3, 15, 21.6, 28.3, 36.3, 44.3, 52.3, and 61.3 min. The H84A data (C) show the appearance of a 344 nm intermediate and a 318 nm intermediate.

Table 4: Results from Global Fitting (SPECFIT/32) of Spectral Changes in the Anaerobic Reaction of PqqC

species	λ_{max} (nm)	ϵ ($mM^{-1}\,cm^{-1}$)[a]	rate constant[b] (min^{-1})
WT-AHQQ	536	2.1	
WT-I_A	318	22	$k_1 = 2.42$ ($\pm$0.07)
WT-I_B	356	12	$k_2 = 1.22$ ($\pm$0.06)
H84N-AHQQ	532	2.1	
H84N-I_A	344	21	$k_2 = 0.80$ ($\pm$0.02)
H84A-AHQQ	532	2.1	
H84A-I_A	344	5.6	$k_1 = 1.57$ (($\pm$0.06)
H84A-I_B	318	31	$k_2 = 0.12$ ($\pm$0.02)

[a] Values for ϵ are all within 5−10%, with the exception of the value for H84A-I_A, which was determined as 5.6 $\pm$ 3.6. [b] Rate constant for formation of species.

(λ_{max} = 366 and 329 nm) appears to be very different from that observed for the WT enzyme; however, incubation of enzyme with authentic PQQ displays the same spectrum, arguing that this chromophore represents enzyme-bound PQQ (see Discussion). The rate of PQQ formation in H84N (0.0562 min^{-1}) is 6-fold slower than for WT, consistent with a proposed role of H84 in the enzymatic reaction (*15*). All three intermediates observed in the reaction have different spectral properties than WT-I. H84N-I_A has a single absorption maximum at 344 nm, whereas H84N-I_B has two maxima at 330 and 448 nm, and H84N-I_C has two maxima at 320 and 445 nm, respectively.

The single-turnover analysis of H84A is simpler than for H84N with the appearance of only two intermediates at 340 and 318 nm. The absence of the third intermediate seen at 330 nm for H84N could have indicated that a three-exponential model is the more appropriate one for H84N. However, as discussed below the anaerobic behavior of the two H84 mutants is quite different. We note that the rate of formation of enzyme-bound PQQ is ca. 2-fold faster for the less conservative mutation, H84A (k = 0.09 min^{-1}), in relation to H84N (k = 0.056 min^{-1}).

Reactions under Anaerobic Conditions. By excluding oxygen from the samples, one can study the initial phases of the PqqC reaction, and Figure 5 shows the spectral changes that occur in the reactions with WT, H84N, and H84A, respectively. The WT reaction displays a time-dependent formation of two independent chromophores with λ_{max} at 318 and 356 nm (Figure 5A) that appear with rate constants of 2.42 $\pm$ 0.07 min^{-1} and 1.22 $\pm$ 0.06 min^{-1}, respectively (see Table 4 and Supporting Information). Exposure of the sample to air yields similar results as when oxygen was present during initiation of the reaction by AHQQ (Figure 2A), indicating that although two species are formed in the absence of oxygen, both can go on to form PQQ.

The H84N reaction performed under anaerobic conditions produces a single chromophore, which persists for hours if oxygen is excluded from the sample (Figure 5B and Table 4). The absorption maximum (344 nm) and extinction coefficient (21 $mM^{-1}\,cm^{-1}$) of the chromophore show that it is H84N-I_A, which is the first species formed in the H84N reaction in the presence of air (Figure 3 and Table 2). Exposure to air leads to the formation of the other two intermediates (H84N-$I_{B/C}$) followed by PQQ (data not shown).

The H84A reaction under anaerobic conditions produces spectra similar to that of the first two intermediates in the

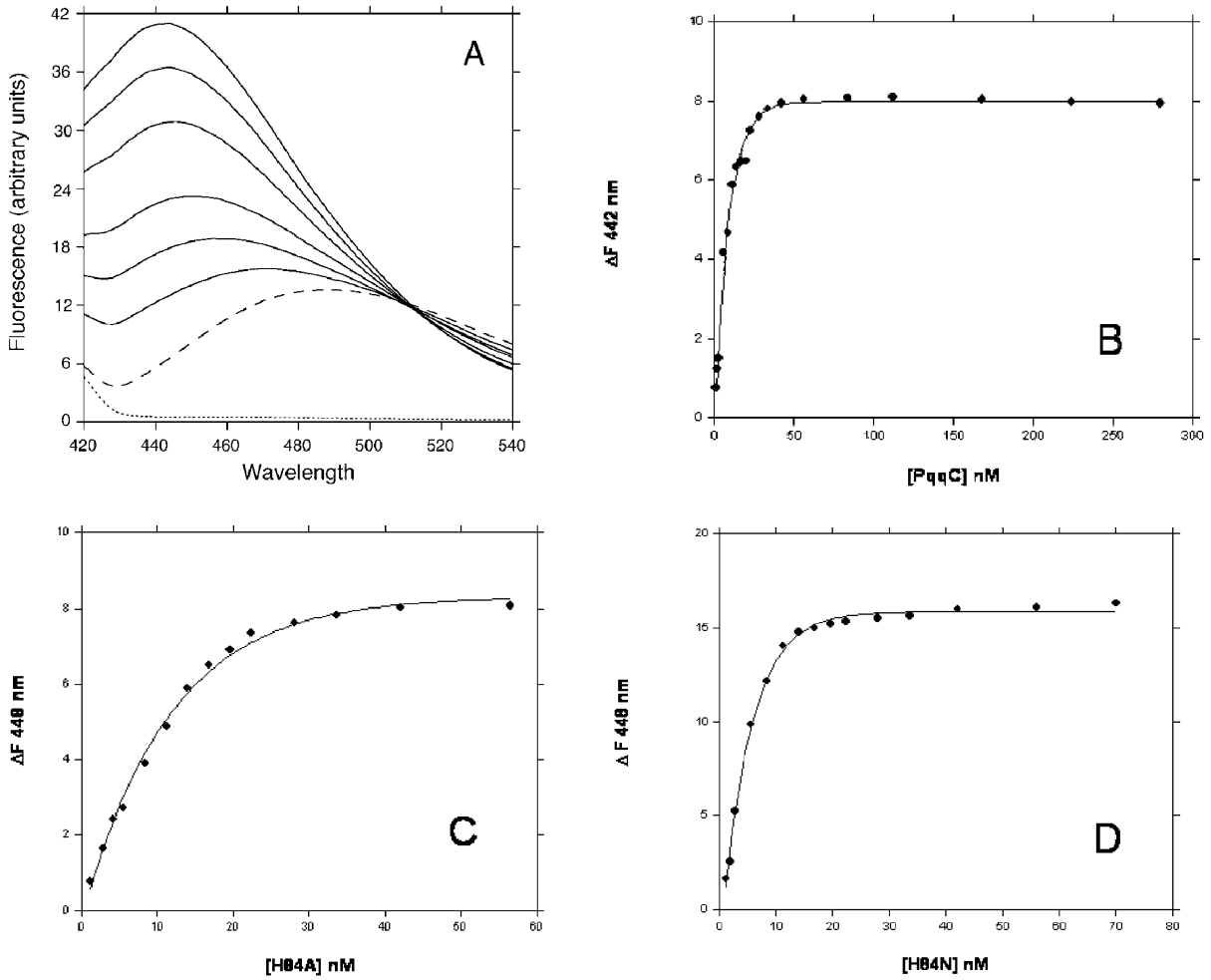

FIGURE 6: Binding of PQQ to WT and H84N form(s) of PqqC as determined by fluorescence spectroscopy. (A) Fluorescence emission spectra of buffer (dotted line), free PQQ (50 nM) (dashed line), and PQQ (50 nM) plus various concentrations of PqqC (solid lines). (B) Binding curve for PQQ (50 nM) binding to WT-PqqC. Data were fitted to eq 1 and yielded a K_D of 2.0 (±0.1) nM. (C) Binding curve for PQQ (20 nM) binding to H84A. Data were fitted to eq 1 and yielded a K_D of 1.7 (±0.2) nM. (D) Binding curve for PQQ (20 nM) binding to H84N. Data were fitted to eq 1 and yielded a K_D of 0.55 (±0.07) nM.

H84A aerobic reaction (Figure 5C and Table 4). However, while the first intermediate (344 nm) has an extinction coefficient similar to the aerobic reaction (Table 3), the 318 nm species has a much lower extinction coefficient. The anaerobic H84A reactions show characteristics of both the H84N and WT reactions: Analogous to H84N, H84A shows an intermediate at 344 nm; however, similar to WT, a species is also observed at 318 nm (Table 4). We note that the extinction coefficients differ among the WT, H84N, and H84A species, with the largest difference seen in the 318 nm peak, observed both aerobically or anaerobically. This could be due to the formation of different quinol species (cf. Scheme 3), to the fact that the SPECFIT analysis is of many overlapping peaks, or a combination of these factors.

Product Binding Studies. PqqC from *K. pneumoniae* and *M. extorquens* are reported to undergo only a single turnover in vitro (*15*, *17*). The addition of an uncharacterized, proteinaceous activating factor and NADPH is reported to result in increased activity of the enzyme, presumably due to multiple turnovers (*17*). In order to study factors leading to the apparent "inactivation" of the enzyme, we have measured the binding affinity of PqqC for PQQ. A sensitive fluorescent assay was developed for the binding process, which takes advantage of a bathochromic shift in the emission spectrum between free PQQ (F_{max} = 488 nm) and enzyme-bound PQQ (F_{max} = 442 nm) and a large increase in fluorescence for the PQQ−PqqC complex compared to free PQQ (Figure 6A). In these experiments, the concentration of PQQ was kept constant at a concentration similar in magnitude to K_D, and the concentration of the enzyme was varied. The data were fitted to a quadratic binding isotherm to derive binding constants (eq 1). Results with WT, H84A, and H84N are shown in panels B, C, and D of Figure 6, respectively. A small hypsochromic shift is observed in the H84N−PQQ or H84A−PQQ complexes (F_{max} = 448 nm) compared to WT−PQQ (F_{max} = 442 nm). The apparent K_D values derived from the data were 2.0 (±0.1) nM for WT, 1.7 (±0.2) for H84A, and 0.55 (±0.07) nM for H84N, which shows that product binding is extremely tight in all cases. These results are perhaps not surprising given the number of interactions in the PqqC−PQQ complex seen in the X-ray crystal structure (*15*).

Activity of PqqC at Lower Protein Concentrations. Previous experiments have indicated that PqqC only undergoes a single turnover (*15*, *17*), suggesting that perhaps inactivation of the enzyme was occurring at the end of the catalytic cycle. These experiments were however done at a relatively high

concentration of enzyme (high nanomolar to micromolar), and the current PQQ binding experiments show that product inhibition is likely to be extremely severe at those concentrations of enzyme. With this in mind, the activity of PqqC under "steady-state" conditions was reexamined. Assays for PqqC were done by quantitating the amount of PQQ formed in the reaction via the PQQ-dependent activation of the apo form of sGDH. This very sensitive assay can detect subnanomolar quantities of PQQ (*20*).

Assays done at 12 μM AHQQ and 2 μM and 105 nM PqqC are shown in panels A and B of Figure 7, respectively. Data obtained under these conditions show that PQQ production ceases at approximately the concentration of enzyme used in the experiments, which means that PqqC is only undergoing a single turnover. In both cases the reaction rate can be fitted to a single exponential with rate constants of $\sim$0.13 min^{-1}. These rate constants are lower than obtained under the single-turnover conditions of Table 1, presumably because the binding of substrate to enzyme has become partially rate-determining. When assays were performed at 4.5 nM PqqC, which is near the estimated K_D of PQQ, the rate behavior was different than before, and the enzyme was able to undergo multiple turnovers (Figure 7C). Examination of the data shows that the reaction rate is linear for approximately 2 turnovers ($\sim$20 min), followed by a decreased rate until formation of PQQ ceases after approximately 7 h of incubation. The drop in rate can presumably be mainly attributed to product inhibition, which becomes significant as the concentration of PQQ exceeds the K_D value for the enzyme−product complex.

DISCUSSION

PqqC catalyzes a complex reaction that involves ring closure via a C−N bond formation followed by an eight-electron oxidation reaction, all in the absence of a metal or organic cofactor (*15*). Under single-turnover conditions, this reaction consumes 3 equiv of O_2, with the remaining two electrons needed to complete the oxidation cycle being used to reduce an intermediate H_2O_2 molecule produced in the enzyme active site. The net reaction is thus the consumption of 3 mol of O_2 and the production of 2 mol of H_2O_2 and 1 mol of H_2O (*15*). The proposed mechanism of PqqC (Scheme 3) shows how the enzyme may facilitate this reaction, by utilizing the inherent chemical reactivity of the substrate to bring about the oxidative chemistry. The first step is illustrated as the ring closure process, followed by O_2-mediated oxidation of the resulting quinol. Although not explicitly shown in Scheme 3, oxidation presumably occurs in two steps in which an outer-sphere electron transfer to O_2 forms as a transient superoxide−semiquinone intermediate prior to quinone and hydroperoxide formation. The subsequent steps are proposed to involve three successive tautomerization reactions (I−III), which serve to activate each of the intermediates for oxidation in the absence of a cofactor. This property of PqqC puts the protein in a small class of enzymes, which carry out oxidative chemistry without the aid of metals or organic cofactors (*21*). What these enzymes have in common is that their respective substrates are already predisposed to react directly with molecular oxygen. Members of this family include urate oxidase (*22*), 1*H*-3-hydroxy-4-oxoquinoline 2,4-dioxygenase (*23*), and ActVA-Orf6 monooxygenase (*24*).

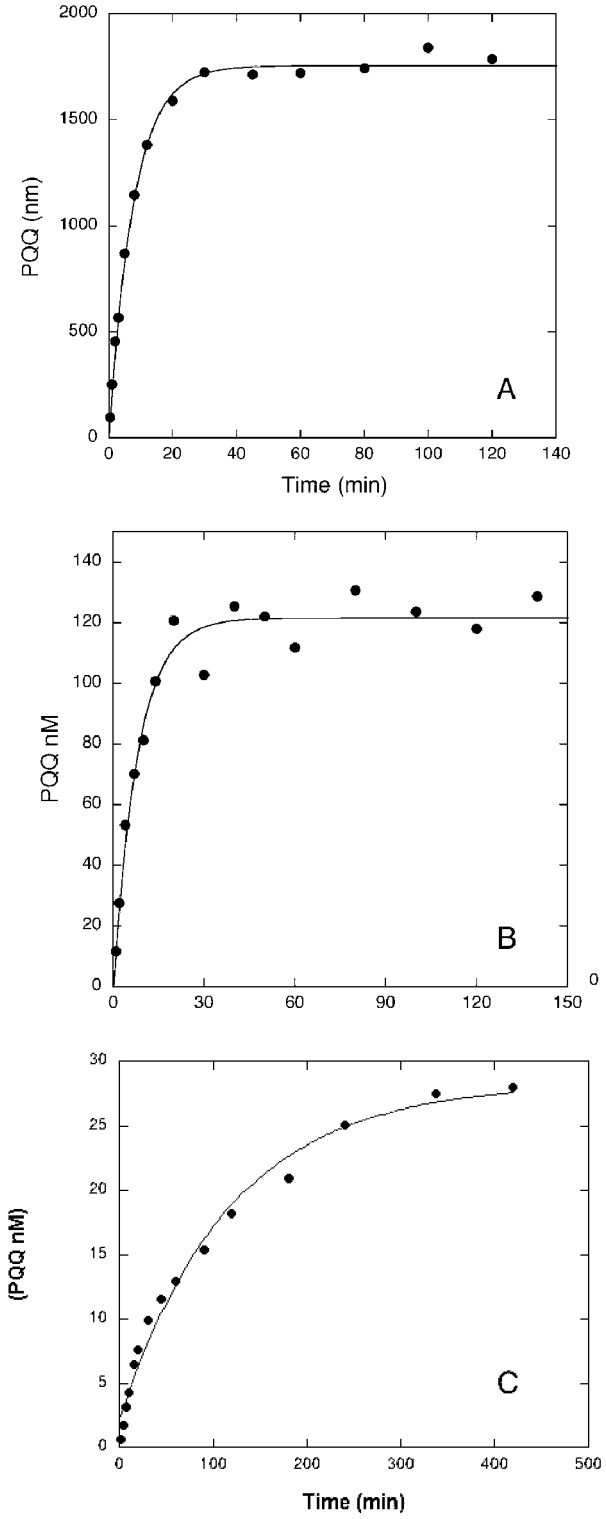

FIGURE 7: Activity of PqqC measured at different concentrations of enzyme. All assays were done in 0.1 M potassium phosphate buffer, pH 8.0, and 12 μM AHQQ at 20 °C. (A) PqqC = 2000 nM. (B) PqqC = 105 nM. (C) PqqC = 4.5 nM.

Single-Turnover Studies in the Presence and Absence of O_2. This study describes the formation and decay of various spectroscopic intermediates on the reaction pathway (Scheme 3). In particular, the function of H84, which is proposed to serve as a general base catalyst and a possible proton donor, has been probed by studying the H84N and H84A variants. The mechanism in Scheme 3 predicts the use of catalytically important basic residues to facilitate the keto−enol tautomer-

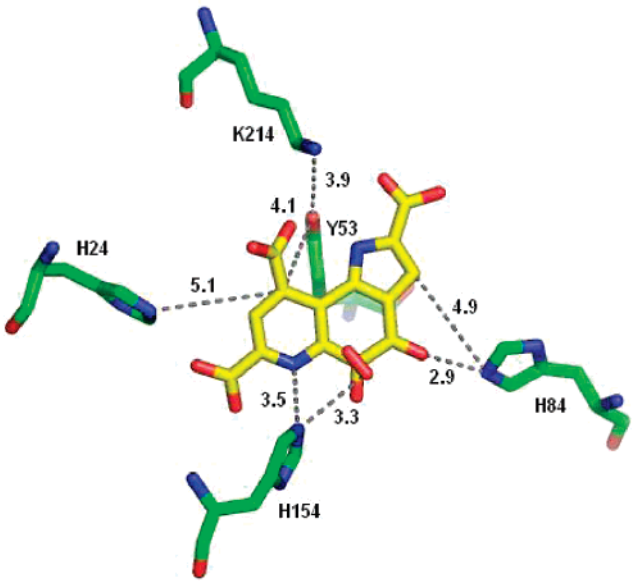

FIGURE 8: Structure and position of proposed catalytic residues in the active site of the PqqC−PQQ complex with the putative oxygen/hydrogen peroxide molecule. The dashed lines show distances in ångstroms between the heavy atoms from which proton transfer reactions occur. These distances are based on the enzyme−product complex and will presumably be somewhat different in the enzyme−substrate complex. Proton transfer at C-9 could be facilitated by either H24 or the Y53/K214 diad.

izations required to activate the substrate for subsequent oxidations. Intermediates shown in brackets in Scheme 3 are believed to be unstable under wild-type conditions and to partition subsequently toward the quinol due to the large driving force of aromatization. The X-ray crystal structure of the PqqC−PQQ complex supports this mechanism (*15*) and presents many interactions that could support the proposed mechanism. Three conserved histidine residues (H84, H154, and H24) are strategically placed to abstract protons at positions C-3, N-6, and C-9, respectively (Scheme 3, Figure 8). H84 is also in a position to interact with the C4 oxygen of bound PQQ, while H154 is within 4 Å of the putative oxygen molecule and could possibly have a role in oxygen binding and reactivity.

Kinetic studies of the WT enzyme under single-turnover conditions show the formation of a single spectroscopic intermediate (WT-I) with λ_{max} at 316 nm. The position and intensity of this band, along with the absence of bands at higher wavelengths, suggest that this intermediate is one of the quinol species on the reaction pathway. The intermediate is formed in a kinetically competent manner (0.96 min^{-1}), i.e., approximately 3-fold faster than PQQ. The rate of formation of PQQ (0.34 min^{-1}) is similar to what has been observed by a different method based on detection of PQQ by HPLC after quenching in acid (0.38 min^{-1}) (*15*). Interestingly, enzyme-bound PQQ displays a bathochromic shift for absorbance of about 15 nm compared to the free cofactor. This shift is likely to result from the electrostatic environment in the enzyme active site, which apparently decreases the energy separation of a π to π^* transition in PQQ.

When the reaction is done anaerobically, two different chromophoric species are observed, with λ_{max} at 318 nm (2.42 min^{-1}) and 356 nm (1.22 min^{-1}), respectively (Figure 5A). Although these chromophores appear at different rates, they

Scheme 4: Proposed Pathway and Accompanying Rate Constants for the Generation of PQQ with WT-PqqC[a]

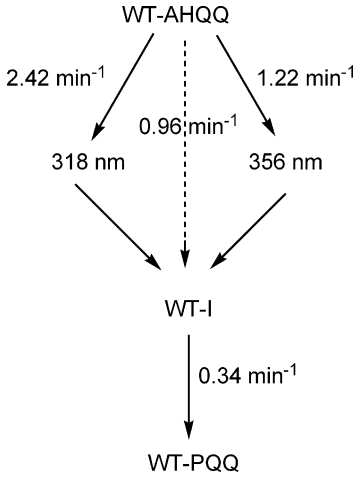

[a] The center line represents the aerobic reaction, and the outer processes are intermediates detected anaerobically.

are both precursors to cofactor as exposure to air leads to formation of WT-I followed by PQQ (data not shown). Scheme 4 depicts the relationship among the species, with the central reaction occurring aerobically and the two side branches representing the anaerobic process. As illustrated, all species are suggested to funnel through WT-I. While the chemical identity of the spectroscopic intermediates remains unproven, the proposed mechanism of the reaction (Scheme 3) allows plausible predictions. The anaerobic reaction prevents oxidation from occurring, such that only an initial quinol species (tentatively assigned to **2** in Scheme 3) would be expected to form. Notice that **2** is drawn in an ionized form, which will undergo reaction with O_2 more rapidly than a fully protonated intermediate. However, the pK_a of the quinol in the active site could be such that under the present experimental conditions this group is only partially deprotonated, hence the two different chromophores for WT-PqqC. The 318 nm species is likely to be the fully protonated quinol, whereas the species at 356 nm is tentatively assigned to monoanionic quinol (Scheme 5).

The reaction of the H84N mutant shows greatly different spectroscopic and kinetic properties than observed for WT. In the presence of O_2, three intermediates (H84N-I_{A-C}) are observed based on global fitting of the data (Figure 3 and Table 2). Importantly, under anaerobic conditions, a sole species is formed, H84N-I_A, with a λ_{max} at 344 nm (Figure 5B and Table 4). The likely identity of the 344 nm species is discussed in greater detail below.

H84N-I_B and -I_C have very similar spectral properties, with both chromophores displaying two transitions above 300 nm, and a signature peak at ~450 nm (Figure 3 and Table 2). The position of the ~450 nm transitions suggests that these could originate from an n to π^* transition of quinone intermediates. The other possibility is that these could represent a semiquinone−superoxide radical pair. Though X-band EPR experiments were unable to detect any signal due to a radical (data not shown), the possibility of strong magnetic coupling between the two radicals rendering the system EPR-silent cannot be ruled out.

Turning to the H84A mutant in the presence of O_2, this shows two intermediates (H84A-I_A and H84A-I_B) before

Scheme 5: Possible Steps of the PqqC Reaction in the Absence of Oxygen[a]

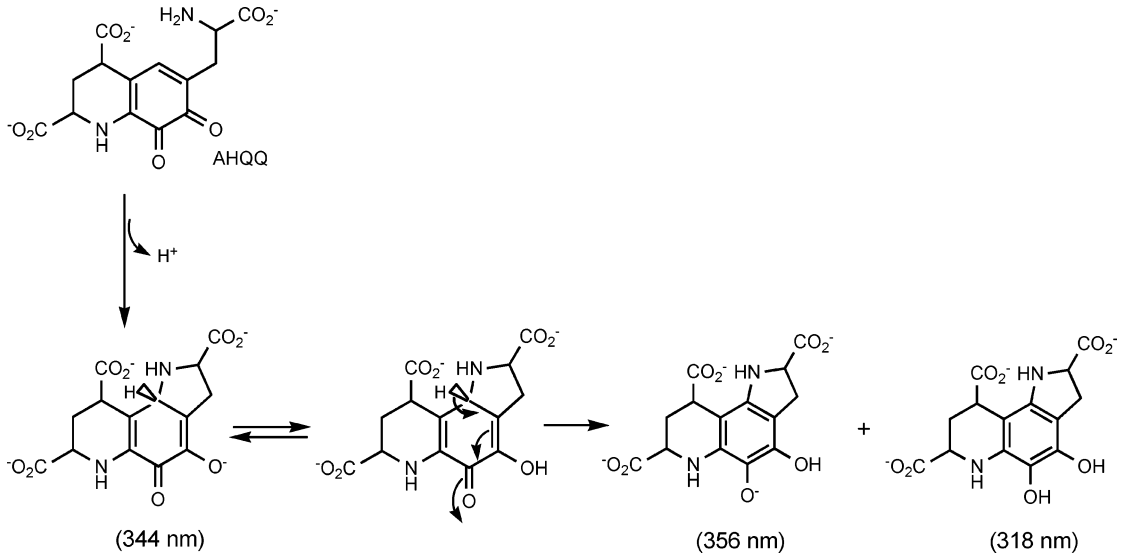

[a] The present analysis assumes that ring closure is the first step. In the wild-type reaction, H84 is proposed to act as a proton donor to the C4 oxygen of the intermediate, allowing the subsequent tautomerization to the quinol to occur. In H84N, there is no proton donor, and so, under anaerobic conditions, protonation and therefore tautomerization cannot occur. In the case of the H84A mutation, space in the active site is proposed to facilitate access of a water molecule that can function as an alternate proton source to bind and act as a proton donor.

product formation (Figure 4 and Table 3). The H84A reaction has properties similar to both the wild-type and H84N reactions. Like H84N, H84A forms PQQ with a blue-shifted absorbance (λ_{max} = 330 and 366 nm). The intermediate seen before PQQ formation (λ_{max} = 318 nm) in the H84A reaction is absent in the H84N reaction, but similar to an intermediate in the wild-type reaction. Under anaerobic conditions, two species are seen in the H84A reaction (Figure 5C). These are quite analogous to what is seen in the aerobic reaction, but do not proceed to product. We note that the first intermediate of both the aerobic and anaerobic H84A reactions (Figure 5C) is similar to that single anaerobic species formed from H84N (λ_{max} = 344 nm) and that no such species is seen in the wild-type reaction. The second intermediate (λ_{max} = 318 nm) is comparable to the anaerobic intermediate found in the wild-type reaction, but is absent from the H84N reaction.

In the anaerobic reaction the final species should be the first quinol species (**2** in Scheme 3), but H84N is only able to form an intermediate at 344 nm. The wild-type reaction forms a species which we believe to be the quinol species at 318 nm. This species is also seen in the H84A reaction, but following a species at 340 nm. It is believed that the mutations cause the formation of the quinol species to be rate-limiting, leading to buildup of a species at approximately 340 nm.

The aggregate spectral data under anaerobic conditions are particularly valuable as they simplify the observed processes and allow us to address the initial series of chemical steps. The band at 318 nm is easily assigned to the fully protonated, first quinol intermediate (Scheme 5) while the band at 344 nm is compatible with a quinoid intermediate (*25*). The fact that H84 is very close (<3 Å) to the C4 oxygen of product (Figure 8) leads us to propose that this histidine acts as a proton donor in the course of the isomerization of the quinoid to quinol intermediates. The finding that H84A can proceed to the first quinol product while H84N cannot requires some structural rationalization. The most likely explanation is that the Ala mutation generates a cavity with enough room for a water molecule to act as a proton donor, while Asn, which is approximately the same size as His, prevents access of water as an alternative proton donor. The kinetic properties of the anaerobic reaction are summarized in the equation:

$$\text{E}-\text{AHQQ} \xrightarrow{k_1} \underset{\text{E}-(\text{quinoid})}{344\text{ nm}} \xrightarrow{k_2} \underset{\text{E}-(\text{quinol})}{318\text{ nm}} \qquad (2)$$

WT: 2.42 min^{-1}	WT: very fast
H84N: 0.80 min^{-1}	H84N: NR
H84A: 1.57 min^{-1}	H84A: 0.12 min^{-1}

As illustrated, the observed rate constant for WT is assigned to k_1, since no 344 nm accumulates, indicating that $k_2 \gg k_1$. The similarity among the k_1 values for WT, H84Q, and H84A indicates that quinoid formation can occur independent of the nature of position 84, while the quinoid to quinol transformation is critically dependent on H84. One notable feature is that H84N turns over to product in the presence of O_2. This suggests structural changes upon O_2 binding that permit proton donation to take place for H84N as well as H84A. We emphasize that while H84 may act as an active site base in PQQ formation (Scheme 3), the anaerobic reaction implicates a key for this residue as a proton donor.

One feature of the aerobic spectra of PQQ in the H84 mutants is a different UV−vis spectrum for the PQQ complexes (Tables 1−3). Although it was possible that the observed complexes were not PQQ, control experiments in which authentic PQQ was added to mutant enzyme yielded the same spectra as observed in the reactions with AHQQ (data not shown). The origin of a large perturbation in the UV−vis spectrum may be explained by the possible presence of a hydrated form of PQQ. In fact, partial hydration occurs in aqueous solution of PQQ at neutral pH (*26*). PQQ−H_2O does not display the weak and broad signature n to π^* transition at ∼480−500 nm, and this transition is also lacking in the mutant−PQQ complexes. Moreover, π to π^* transi-

tions of PQQ−H_2O in solution are observed at ∼330 and 360 nm (*26*), which is similar to what is seen for the mutant−PQQ product complexes. We, therefore, propose that H84 mutations shift the population of bound product toward the hydrated form of PQQ.

Tight Binding of PQQ Affects Turnover Kinetics. Fluorescence titration experiments show that PQQ binds its product very tightly. The binding constant is only 2.0 nM, and, perhaps somewhat surprisingly, the binding affinity is not compromised in the H84N mutant (0.55 nM) or the H84A mutant (1.7 nM). The tight binding of PQQ can explain why enzymatic assays of PqqC had been unable to detect more than a single turnover. In these assays the concentration of PqqC was typically in the high nanomolar or low micromolar range such that PQQ formed in the reaction remained tightly bound at the active site (Figure 7A,B). By lowering the concentration of enzyme below the K_D, a different result is obtained, where approximately 6 enzyme turnovers can be detected (Figure 7C). Further analysis to measure kinetic parameters (k_{cat}/K_M) is currently underway; however, these experiments are complicated due to the low reactivity of PqqC and sensitivity of the enzymatic assay (sGDH), which is employed to detect PQQ.

CONCLUSIONS

The data described herein provide important information regarding the mechanism of PqqC, including the spectral detection of several intermediates in the catalytic cycle. The role of one putative catalytic residue (H84) has been probed, leading to its proposed role as a general acid catalyst in the conversion of quinoid to quinone species. Ongoing mutagenesis studies of the additional basic residues surrounding the substrate are expected to provide insight into the nature of additional chemical intermediates formed during the extremely complex reaction catalyzed by PqqC. The demonstrated tight binding of PQQ at the active site of PqqC raises the question of how this enzyme can catalyze multiple turnovers in vivo. Additionally, although PQQ is formed in the cytosol Gram-negative bacteria, it must be delivered to the periplasm before it can function. Ongoing studies are addressing whether proteins encoded within in the PQQ operon function to facilitate release of PQQ from PqqC and the delivery of PQQ to the periplasmic space.

SUPPORTING INFORMATION AVAILABLE

A standard curve for the assay of PQQ concentration using glucose dehydrogenase, a summary of data obtained from global fitting of the aerobic WT-PqqC reaction, a comparison of three- versus four-exponential fitting in the aerobic H84N reaction, and rates for formation of spectroscopic intermediates in the WT-PqqC reaction under anaerobic conditions. This material is available free of charge via the Internet at http://pubs.acs.org.

REFERENCES

1. Anthony, C. (2001) Pyrroloquinoline quinone (PQQ) and quinoprotein enzymes, *Antioxid. Redox Signaling 3*, 757−774.
2. Goodwin, P. M., and Anthony, C. (1998) The biochemistry, physiology and genetics of PQQ and PQQ-containing enzyme, *Adv. Microb. Physiol. 40*, 1−80.
3. Duine, J. A. (2001) Cofactor diversity in biological oxidation; implications and applications, *Chem. Rec. 1*, 74−83.
4. He, K., Nukada, H., Urakami, T., and Murphy, M. P. (2003) Antioxidant and pro-oxidant property of pyrroloquinoline quinone (PQQ): implications for its function in biological systems, *Biochem. Pharmacol. 65*, 67−74.
5. Mitchell, A. E., Jones, A. D., Mercer, R. S., and Rucker, R. B. (1999) Characterization of pyrroloquinoline quinone amino acid derivatives by electrospray ionization mass spectrometry and detection in human milk, *Anal. Biochem. 269*, 317−325.
6. Steinberg, F., Stites, T. E., Anderson, P., Storms, D., Chan, I., Eghbali, S., and Rucker, R. (2003) Pyrroloquinoline quinone improves growth and reproductive performance in mice fed chemically defined diets, *Exp. Biol. Med. (Maywood, NJ) 228*, 160−166.
7. Kasahara, T., and Kato, T. (2003) A new redox-cofactor vitamin for mammals, *Nature 422*, 832.
8. Felton, L. M., and Anthony, C. (2005) Role of PQQ as a mammalian enzyme cofactor, *Nature 433*, E10.
9. Unkefer, C. J. (1993) in *Principles and Applications of Quinoproteins* (Davidson, V. L., Ed.) pp 343−353, Marcel Dekker, New York.
10. Goosen, N., Huinen, G. R. M., and van de Putte, P. (1992) A 24-amino acid polypeptide is essential for the biosynthesis of the coenzyme pyrroloquinoline quinone, *J. Bacteriol. 174*, 1426−1427.
11. Meulenberg, J. J., Sellink, E., Riegman, N. H., and Postma, P. W. (1992) Nucleotide sequence and structure of the *Klebsiella pneumoniae pqq operon*, *Mol. Gen. Genet. 232*, 284−294.
12. Velterop, J. S., Sellink, E., Meulenberg, J. J., David, S., Bulder, I., and Postma, P. W. (1995) Synthesis of pyrroloquinoline quinone *in vivo* and *in vitro* and detection of an intermediate in the biosynthetic pathway, *J. Bacteriol. 177*, 5088−5098.
13. Toyama, H., Chistoserdova, L., and Lidstrom, M. E. (1997) Sequence analysis of pqq genes required for biosynthesis of pyrroloquinoline quinone in *Methylobacterium extorquens* AMI and the purification of a biosynthetic intermediate, *Microbiology 143*, 595−602.
14. Magnusson, O. Th., Toyama, H., Saeki, M., Schwarzenbacher, R., and Klinman, J. P. (2004) The structure of biosynthetic intermediate of pyrroloquinoline quinone (PQQ) and elucidation of the final step of PQQ biosynthesis, *J. Am. Chem. Soc. 126*, 5342−5343.
15. Magnusson, O. Th., Toyama, H., Saeki, M., Rojas, A., Reed, J. C., Liddington, R. C., Klinman, J. P., and Schwarzenbacher, R. (2004) Quinone biogenesis: structure and mechanism of PqqC, the final catalyst in the production of pyrroloquinoline quinone, *Proc. Natl. Acad. Sci. U.S.A. 101*, 7913−7918.
16. Schwarzenbacher, R., Stenner-Liewen, F., Stenner, H., Reed, J. C., and Liddington, R. C. (2004) Crystal structure of PqqC from *Klebsiella pneumoniae* at 2.14 Å resolution, *Proteins 56*, 401−403.
17. Toyama, H., Fukumoto, H., Saeki, M., Matsushita, K., Adachi, O., and Lidstrom, M. E. (2002) PqqC/D which converts a biosynthetic intermediate to pyrroloquinoline quinone, *Biochem. Biophys. Res. Commun. 299*, 268−272.
18. Duine, J. A., Frank, J., and Jongejan, J. A. (1987) Enzymology of quinoproteins, *Adv. Enzymol. 59*, 170−212.
19. Olsthoorn, A. J. J., and Duine, J. A. (1996) Production, characterization and reconstitution of recombinant quinoprotein glucose dehydrogenase apoenzyme of *Acinetobacter calcoaceticus*, *Arch. Biochem. Biophys. 336*, 42−48.
20. Matsushita, K., Toyama, H., Ameyama, M., Adachi, O., Dewanti, A., and Duine, J. A. (1995) Soluble and membrane-bound quinoprotein D-glucose dehydrogenases of *Acinetobacter calcoaceticus:* the binding process of PQQ to the apoenzyme, *Biosci., Biotechnol., Biochem. 59*, 1548−1555.
21. Fetzner, S. (2002) Oxygenases without requirement for cofactors or metal ions, *Appl. Microbiol. Biotechnol. 60*, 243−257.
22. Kahn, K., and Tipton, P. A. (1998) Spectroscopic characterization of intermediates in the urate oxidase reaction, *Biochemistry 37*, 11651−11659.
23. Fischer, F., and Fetzner, S. (2000) Site-directed mutagenesis of potential catalytic residues in 1H-3-hydroxy-4-oxoquinoline 2,4-dioxygenase, and hypothesis on the catalytic mechanism of 2,4-dioxygenolytic ring cleavage, *FEMS Microbiol. Lett. 190*, 21.

24. Sciara, G., Kendrew, S. G., Miele, A. E., Marsh, N. G., Federici, L., Malatesta, F., Schimperna, G., Savino, C., and Vallone, B. (2003) The structure of ActVA-Orf6, a novel type of monooxygenase involved in actinorhodin in biosynthesis, *EMBO J. 22*, 205−215.
25. Nabiullin, A. A., Fedoreev, S. A., and Deshko, T. N. (1984) Circular dichroism of quinoid pigments from Far Eastern representatives of the family Boraginaceae, *Chem. Nat. Compd. 19*, 532−537.
26. Dekker, R. H., Duine, J. A., Frank, J., Eugene, J. P., Verwiel, J., and Westerling, J. (1982) Covalent addition of water, enzyme substrates, *Eur. J. Biochem. 125*, 69−73.
27. Ohshiro, Y., and Itoh, S. (1993) in *Principles and Applications of Quinoproteins* (Davidson, V. L., Ed.) p 313, Marcel Dekker, New York.

BI700162N